



Contents lists available at ScienceDirect

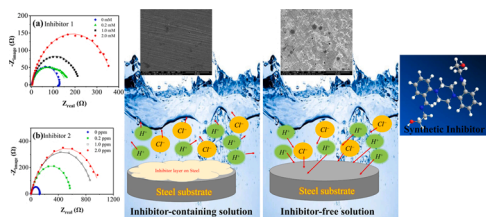
Colloids and Surfaces A: Physicochemical and Engineering Aspects

journal homepage: www.elsevier.com/locate/colsurfa

Experimental and theoretical investigation of corrosion inhibition effect of two piperazine-based ligands on carbon steel in acidic media

Majid Rezaeivala^{a,*}, Saeid Karimi^{b,*}, Koray Sayin^c, Burak Tüzün^c^a Department of Chemical Engineering, Hamedan University of Technology, Hamedan 6516913733, Iran^b Department of Metallurgy and Materials Engineering, Hamedan University of Technology, Hamedan 6516913733, Iran^c Chemistry Department, Science Faculty, Sivas Cumhuriyet University, 58140 Sivas, Turkey

GRAPHICAL ABSTRACT



ARTICLE INFO

Keywords:

Schiff base
Piperazine
Acid corrosion
EIS
Electrochemistry
Acid inhibition
Carbon steel, DFT
Theoretical calculation, protonated form

ABSTRACT

In this study, the corrosion of carbon steel in 1.0 M HCl solutions containing either 1,4-bis(2-(2-hydroxyethyliminomethyl)phenyl)piperazine (1) or its reduced form, 1,4-bis(2-(2-hydroxyethylaminomethyl)phenyl)piperazine (2), as possible corrosion inhibitors, were compared to a solution containing no (1) or (2). The various concentrations of inhibitors, 0.2, 1.0, and 2.0 mM, were used to explore the inhibition ability of the synthesized materials against carbon steel corrosion. The morphology and chemical analysis of the as-received and corroded samples were investigated by scanning electron microscopy (SEM) and energy-dispersive X-ray spectroscopy (EDS). By assessing potentiodynamic data, the i_{corr} of carbon steel electrode is the highest value among the other inhibitor-containing solutions, demonstrating a minimum corrosion resistance in 1.0 M HCl solution. While, the protection of carbon steel (1) and (2)-containing solution increased by raising the concentration of (1) and (2) from 0.2 to 2.0 mM. The reduced form of (1) showed a superior corrosion resistance for carbon steel compared to inhibitor (1). The corrosion efficiency of carbon steel in 1.0 M HCl attained a maximum value of 66.08% for inhibitor (1) and 88.51% for inhibitor (2) when the concentration of inhibitor reached the highest value. The results obtained from electrochemical impedance spectroscopy, EIS, illustrated that the capacitance of the double layer, C_{dl} , decreased with an increment of inhibitor (1) and (2) concentration, while the charge transfer resistance of carbon steel enhanced as the inhibitor increased. SEM images reveals that the carbon steel had a severe corrosion inhibitor-free solution, while the surface in inhibitor (1) and (2)-containing solution looks more smooth and uniform. The obtained results in EIS and Tafel measurements were clearly consistent with our observation in the SEM images. According proposed inhibition mechanism, the inhibitor adsorption on the carbon steel prevents the hydrogen evolution from the cathodic sites and dissolution of iron in the anodic regions. Adsorption of both inhibitors, (1) and its reduced form (2), was found to obey the Temkin adsorption

* Corresponding authors.

E-mail addresses: mrezaeivala@hut.ac.ir (M. Rezaeivala), s.karimi@hut.ac.ir (S. Karimi).<https://doi.org/10.1016/j.colsurfa.2022.128538>

Received 14 October 2021; Received in revised form 2 February 2022; Accepted 4 February 2022

Available online 8 February 2022

0927-7757/© 2022 Elsevier B.V. All rights reserved.

isotherm. The inhibitory properties of inhibitor molecules have also been studied by theoretical calculations, using Gaussian 09 software program, enabling a comparison of the properties of (1) and (2).

1. Introduction

Carbon steel is one of the most widely used alloys in the construction and petroleum production industries on account of its strength, cost-effectiveness, technical efficiency and availability. Prevention of corrosion is one of the most challenging issues relating to selection of materials for various purposes in many different industries. Therefore, it is paramount that engineers and scientists not only investigate the corrosion mechanism of carbon steel in different solutions, but also have the final goal of being able to determine the most efficient approach in minimizing corrosion [1–3]. In recent years, the use of inhibitors against the corrosion of steel has been the subject of much attention and study owing to there being a significant reduction of corrosion of the steel when immersed in solutions containing chloride ions in the presence of inhibitors [4–7]. The mechanism of resistance of carbon steel to corrosion in inhibitor-containing solutions is well understood to be due to the inhibitors being adsorbed onto the surface of the steel displacing any corrosive species [8]. The inhibition efficiency of inhibitors against the corrosion of carbon steel in harsh corrosive solutions is strongly related to the molecular structure, functional groups and chemical compositions of the inhibitors [3].

Organic inhibitors containing heteroatoms (such as oxygen, nitrogen or sulfur) are the most efficient compounds in inhibiting corrosion [8]. In spite of there being many research papers on the effects of inhibitors on the corrosion of carbon steel [9–11] there is still an uncertainty about using the inhibitors on an industrial-scale, especially in the oil and gas production industries, due to the different corrosion behaviors in different industrial processes, the limitations in the practical application of inhibitors and the specific nature of many organic inhibitors [12]. It is therefore necessary to develop and study new inhibition compounds to minimize the risks in the selection and application of inhibitors in minimizing corrosion in various industrial processes. Inhibitors containing nitrogen, like benzotriazole and triazole, have been intensively used to protect carbon steel, zinc, and aluminum and copper alloys [13–16]. It has been found that organic inhibitors having many nitrogen heteroatoms, which are able to donate electron pairs to the carbon steel, could enhance the inhibition efficiency [17]. This is consistent with increasing the nitrogen chain length in the organic compounds to increase surface protection from corrosion. As well, the insufficient hydrolytic stability of most of the inhibitors in sulfuric acid and hydrochloric acid can be increased by reduction methods [12,18–20]. Table 1 has shown the different inhibitors containing piperazine and their inhibition efficiency in different acidic solutions. As can be seen in Table 1, these type inhibitors can be used in different range of acidic solutions and metal or alloys (e.g. steel and copper) with an excellent efficiency 96.6% and a minimum at 82.4%.

Schiff base compounds are used in variety range of applications [27] such as anti-corrosion [28–30], anti-cancerous [31,32], anti-bacterial and anti-fungal material [33–35] and DNA cleavage [36]. A survey of literature demonstrates that the Schiff base compound is an effective inhibitor in corrosive media, like 4-(((4-(bis(pyridin-2-ylmethyl) amino) phenyl) imino) methyl)-N,N-diethylaniline [28], benzaldehyde (CSB-1), 4-(dimethylamino)benzaldehyde (CSB-2), and 4-hydroxy-3-methoxybenzaldehyde (CSB-3) [37] and three Schiff base compounds [29]. Ji et al. [28] have found that BPMA inhibitor efficiency can be reach c.a. 88.2% at concentration of 1.0 mM for mild steel in 1.0 M HCl. While, Elemike et al. [29] have reported that the corrosion efficiency of TMPOL, BMPOL and PMPOL (Schiff base compounds inhibitor) can reach a maximum of 75%, 88% and 74%, respectively. They claim that the existence of a methylene linkage increase the donor-acceptors on the mild steel surface. Schiff base compounds demonstrate an excellent

protection from corrosive media at very low level of concentration. While, several studies have been worked on the anti-corrosion of Schiff base compounds. Recently we have reported the synthesis of a new Schiff base ligand containing morpholine moiety and related reduce form as a good corrosion inhibitor for mild steel in 1.0 M HCl solution [38].

The mechanism of inhibitor molecules protection has been investigated in term of free electrons in p orbital, the electron density around N-containing molecules and the number of electron pairs on the steel surface [39]. An adsorption of organic inhibitor molecules on the steel surface is accomplished by a substitution of adsorbed H_2O_{ads} with inhibitors (inh_{ads}). Adsorption of the inhibitor on metal surface depends on different parameters such the physicochemical properties, the electrolyte and electric charge of metal surface [40]. Also, it has been reported that the adsorbed inhibitor can only decrease the active carbon steel surface in acidic solution, in which the mechanism of anodic dissolution of electrode and hydrogen evaluation on cathodic site did not change [28]. The value of standard free energy of adsorption (ΔG^0_{ads}) is a sign for selection the inhibition mechanisms on the metals. If the high absolute value of ΔG^0_{ads} indicates the strong bonding between the carbon steel surface and inhibitor species, indicating a chemical adsorption of inhibitor molecules. While, the minimum one for ΔG^0_{ads} reveals that the physical adsorption occurred on the metal surface [28]. It should be noted that both mechanisms of chemical and physical adsorption can take place spontaneously on the carbon steel surface [41].

In the present study, the corrosion inhibition of carbon steel in 1.0 M HCl solutions containing inhibitor (1) and its reduced form (2) was studied using electrochemical measurements (polarization and EIS tests). Theoretical calculations can be used as an important guide for many experimental studies. There are many quantum chemical parameters related to inhibitor molecules that can be determined and so these calculations can be used to quickly and easily compare the inhibitory activities of inhibitor molecules. For inhibitor molecule (1) and its reduced form (2) these quantum chemical parameters were calculated using the B3LYP, HF, and M062X level 6–31 + +G(d,p) basis set with the Gaussian software program, thus enabling a theoretical comparison of inhibitor molecules and their protonated form [42,43].

2. Experimental

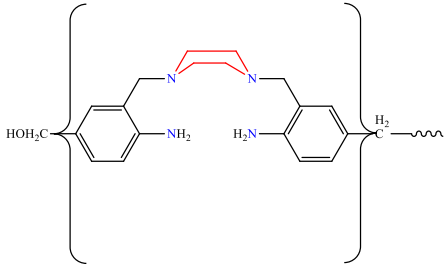
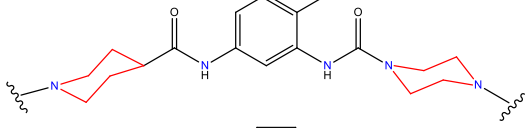
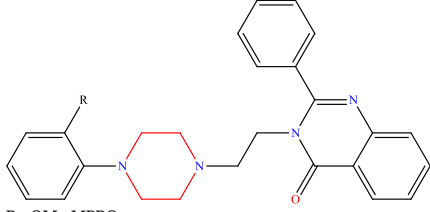
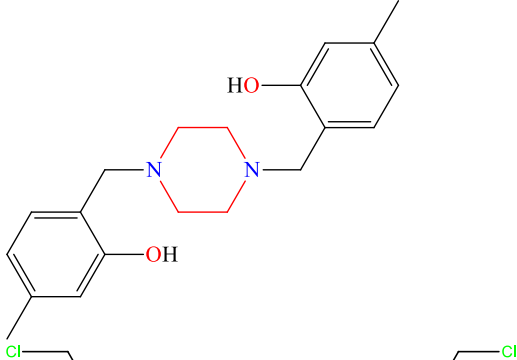
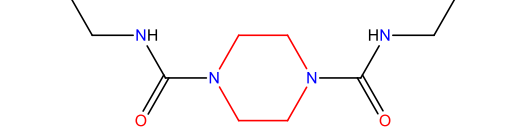
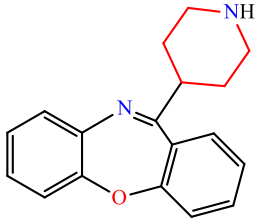
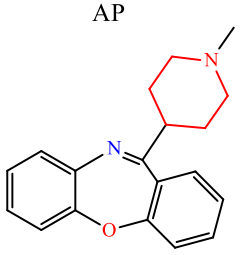
1,4-Bis(2-formylphenyl)piperazine was prepared according to the literature method [44,45]. Infrared (IR) spectra were collected on a BIO-RAD FTS-40A spectrophotometer ($4000\text{--}400\text{ cm}^{-1}$). Nuclear magnetic resonance (NMR) spectra were recorded on a Bruker 500 spectrometer operating at 500.06 MHz, respectively. Mass spectra were measured on a Bruker micro TOFQ. Standard microanalysis for all complexes was carried out using a CHNS/O elemental analyzer (model 2400, Perkin-Elmer).

2.1. Synthesis

2.1.1. Synthesis of 1,4-bis(2-(2-hydroxyethyliminomethyl)phenyl)piperazine (1)

1,4-Bis(2-formylphenyl)piperazine (0.588 g, 2 mmol) and 2-aminoethanol (0.244 g, 4 mmol) were mixed in ethanol (30 ml). The stirred mixture was refluxed for 2 h. The solution was filtered and the filtrate volume was reduced to ca. 10 ml. The obtained compound was washed with ethanol and dried in vacuo. Yield: 88%. For $C_{22}H_{28}N_4O_2$: Anal. Calcd. (%), C:69.45; H, 7.42; N, 14.73. Found, (%): C, 69.86; H, 7.40; N, 14.90. EI-MS (m/z): found (calcd): 380.00 (380.48) $[L]^+$. IR (ATR, cm^{-1}):

Table 1
Different inhibitors containing piperazine and their inhibition efficiencies.

Inhibitors	Inhibition efficiencies (%)	Electrolyte	Alloy or metal	Ref.
	98.00	1 M HCl	Mild steel	[21]
	94.5	0.5 M NaCl	Mild steel	[22]
 <p>R=H PPQ</p> <p>R=OMe MPPQ</p>	96.1	1.0 M HCl	Mild steel	[23]
	96.6 93.5	0.2 M H ₂ SO ₄	Mild steel	[24]
	82.4	0.5 M HCl	Mild steel	[25]
	94.0	0.5 M H ₂ SO ₄	Copper	[26]
 <p>AP</p> <p>LP</p>	95.2			

(continued on next page)

3218 (OH), 1645 (C=N Schiff base), 1486 (C=C). ^1H NMR (CDCl_3 , ppm): $\delta = 3.18$ (s, 8 H, H-a), 3.80 (t, 4 H, H-c), 3.92 (t, 4 H, H-b), 7.15 (d, 2 H, H-e), 7.17 (t, 2 H, H-g), 7.44 (t, 2 H, H-f), 7.93 (d, 1 H-H-h), 8.75 (s, 2 H, H-j). ^{13}C NMR (CDCl_3 , ppm): $\delta = 53.42$ (c-a), 61.42 (c-c), 61.88 (c-b), 118.90 (c-g), 123.45 (c-e), 128.06 (c-i), 129.42 (c-i), 131.46 (c-f), 152.75 (c-d), 161.56 (c-j) (Scheme 1).

2.1.2. Synthesis of 1,4-bis(2-(2-hydroxyethylaminomethyl)phenyl)piperazine (2)

To an ethanolic solution (50 ml) of (1) (0.5 mmol, 0.239 g) was slowly added sodium borohydride (0.25 mmol, 0.009 g). The mixture was stirred and heated to reflux for 12 h. A brown oil was obtained that was filtered off, washed with cold ethanol and dried in vacuo. Yield: 85%. For $\text{C}_{22}\text{H}_{32}\text{N}_4\text{O}_2$: Anal. Calcd. (%), C:68.72; H, 8.39; N, 14.57. Found, (%): C, 68.86; H, 8.20; N, 14.75. EI-MS (m/z): found (calcd): 383.41 (384.51) $[\text{L}-1]^+$. IR (ATR, cm^{-1}): 3294 $\nu(\text{OH})$, 3119 $\nu(\text{N-H})$, 1598 $\nu(\text{C=N})$, 1492 $\nu(\text{C=C})$. ^1H NMR (CDCl_3 , ppm): $\delta = 2.60$ (t, 2 H, H-e'), 2.81 (t, 4 H, H-b'), 3.11 (s, 8 H, H-a'), 3.70 (t, 4 H, H-c'), 3.92 (s, 4 H, H-d'), 7.13 (t, 2 H, H-i'), 7.24 (d, 2 H, H-g'), 7.30 (t, 2 H, H-h'), 7.35 (d, 2 H, H-j'). ^{13}C NMR (CDCl_3 , ppm) $\delta = 49.79$ (c-d), 50.86 (c-b), 53.40 (c-a), 60.99 (c-c), 120.56 (c-g), 124.34 (c-i), 128.13 (c-k), 129.99 (c-j), 134.93 (c-h), 151.52 (c-f) (Scheme 1).

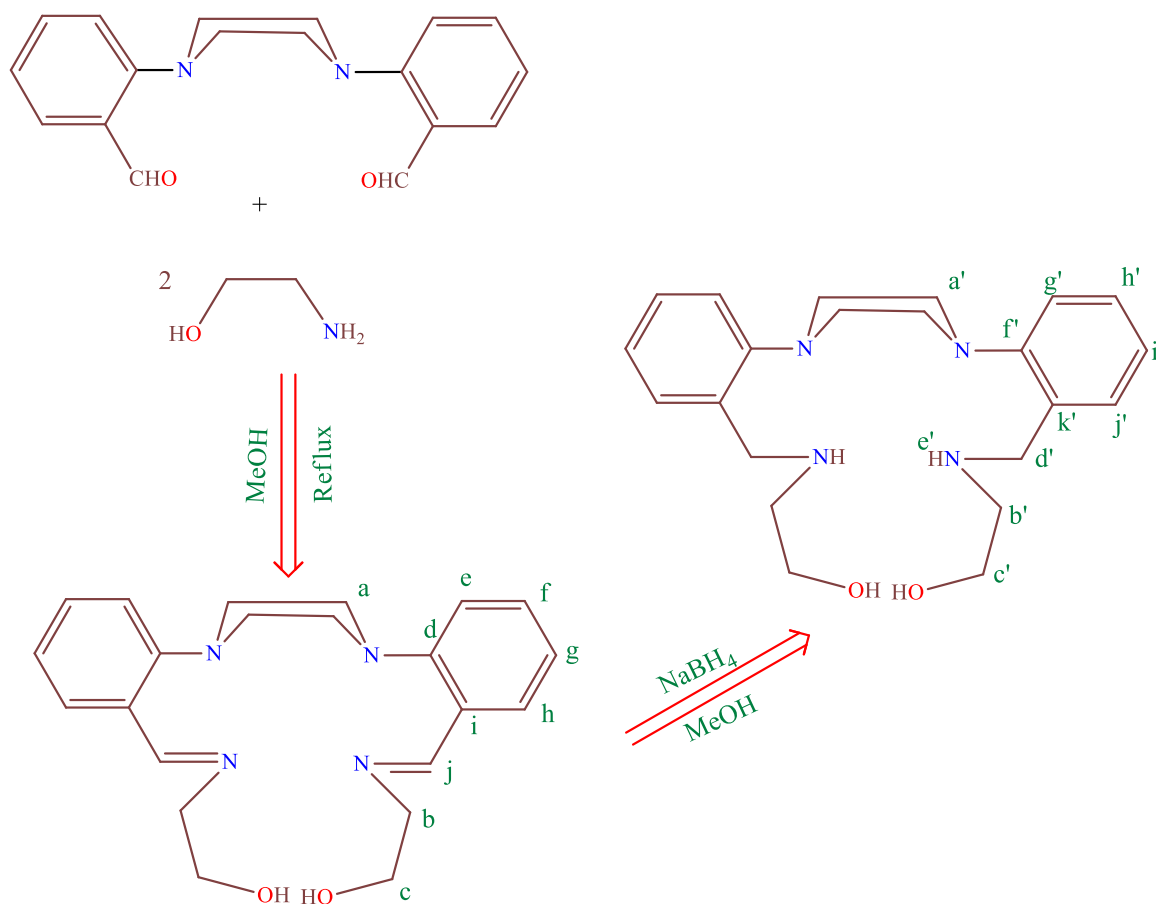
2.2. Electrochemical measurement

The corrosion inhibition performance of two piperazine of 1,4-bis(2-

(2-hydroxyethyliminomethyl)phenyl)piperazine (1) and its reduced form, 1,4-bis(2-(2-hydroxyethylaminomethyl)phenyl)piperazine (2), were measured by electrochemical techniques, including Tafel and electrochemical impedance spectroscopy (EIS). The conventional three-electrode-electrochemical cell using a Iviumstat compact 20250 H potentiostat, controlled by Ivium electrochemistry software, and a GSTAT101N Potentiostat (Metrohm Autolab) controlled by Nova software (Version 2.1.4) were used. The chemical composition of carbon steel, was used as the working electrode, is (wt%) 0.049 C, 0.010 Si, 0.003 Ni, 0.221 Mn, 0.013 P and 0.001 Cr. A platinum electrode with large surface area as counter electrode and an Ag/AgCl electrode (Metrohm) filled with 3.5 M KCl (217 mV vs. SHE at 22 °C) as reference electrode was employed in electrochemical measurements. Each electrochemical testing was conducted on the carbon steel with a surface area of 1 cm^2 at room temperature. Before electrochemical measurements, the working electrodes were ground wet to 1000–1500 grits SiC and then rinsed with acetone and finally dried in hot air. The analytical grade of hydrochloric acid (purity 37%) was used to prepare the testing solution with a concentration of 1.0 M. The concentration of inhibitors (1) and its reduced form (2) were varied within the range of 0.0–2.0 mM to verify the inhibitor effect on the corrosion of carbon steel. The OCP measurements were initially recorded for 20 min in inhibitor-free and inhibitor-containing solution until a stable potential was reached. The Tafel tests were measured within the potential range of ± 0.70 V vs. OCP at a constant scan rate of 1 mV/s and converted to current density by figuring the surface area. Electrochemical impedance spectroscopy (EIS)

Table 1 (continued)

Inhibitors	Inhibition efficiencies (%)	Electrolyte	Alloy or metal	Ref.
	96.6			
CP 	83	5.5 M H_3PO_4	C38 steel	[27]
	97			
	98.8	4 M HCl	13Cr steel	[28]



Scheme 1. Synthesis of inhibitors (1) and (2).

tests were conducted in the inhibitor-free and inhibitor-containing of 1.0 M HCl solution at OCP. The frequency range was 10^{-1} - 10^5 Hz with peak-to-peak amplitude of 10 mV. Each electrochemical experiment was repeated at least twice to ensure the reproducibility of results. In addition, all electrochemical experiments were performed in the stagnant condition, where the results can be compared with experiments published by another studies [46,47].

2.3. Surface characterization using SEM and EDS

A FEI Quanta 450 scanning electron microscope (SEM) equipped with energy-dispersive X-ray spectroscopy (EDS) was used to survey the morphology and composition of carbon steel surface. The steel specimen were cut into $1.0 \times 1.0 \times 1.0$ cm³ samples and then, were polished on emery papers of 400, 800, 1000 and 2000 grade. Then, the carbon steel was washed twice times with distilled water and rinsed with ultrapure acetone, respectively. To survey the inhibiting performance, the samples were dipped in 1.0 M HCl solutions with (inhibitor (1) or (2)) and without 2.0 mM inhibitors for 24 h at room temperature (22 °C). Finally, the samples rinsed by distilled water several times followed by acetone to remove any particles on the surface.

2.4. DFT calculation

The Gaussian 09 software program [48] was used to compare the theoretical activities of the inhibitor molecules. The structures were optimized using the B3lyp [49–51], HF [52], and M062X [53] methods and 6-31 + +G(d, p) basis set. A number of quantum chemical parameters were calculated including E_{HOMO} , E_{LUMO} , ΔE (HOMO-LUMO energy gap), electronegativity (χ), chemical potential (μ), chemical hardness (η), electrophilicity (ω), nucleophilicity (ϵ), global softness (σ)

and proton affinity (PA) [54,55].

$$\eta = - \left(\frac{\partial^2 E}{\partial N^2} \right)_{v(r)} = \frac{1}{2}(I - A) \cong -\frac{1}{2}(E_{HOMO} - E_{LUMO}) \quad (1)$$

$$\sigma = 1/\eta \quad \omega = \chi^2/2\eta \quad \epsilon = 1/\omega \quad (2)$$

3. Result and discussion

3.1. Characterization of 1,4-bis(2-(2-hydroxyethyliminomethyl)phenyl)piperazine (1) and 1,4-bis(2-(2-hydroxyethylaminomethyl)phenyl)piperazine (2)

3.1.1. FT-IR and Mass spectra

A Schiff base ligand (1) has been prepared through the condensation reaction of 1,4-bis(2-formylphenyl) piperazine and ethanolamine, with a molar ratio of 1:2, for 6 h in ethanol. The prepared Schiff base was characterized by microanalysis and by spectroscopic techniques. The FT-IR spectrum of the Schiff base ligand (1), showed a sharp band at 1645 cm⁻¹ related to the stretching vibration frequency of the imine group, indicating the condensation of the precursors to produce the Schiff base ligand. The mass spectrum of (1) showed the molecular ion peak at $m/z = 380$ which is consistent with the proposed molecular formula. Compound (2) was prepared by an in-situ reduction of the Schiff-base ligand, and characterized by microanalysis, IR, EI-MS and ¹H and ¹³C NMR spectroscopy. The IR spectrum shows bands at 1598, 1569 and 1479 cm⁻¹, associated with the $\nu(C=N)$ and $\nu(C=C)$ vibrations from the pyridine ring. The $\nu(N-H)$ band appears at 3119 cm⁻¹. The mass spectrum of (2) showed the molecular ion peak at $m/z = 383.41$ which is consistent with the proposed molecular formula.

3.1.2. NMR spectral studies

The ^1H and ^{13}C NMR spectra of the compounds were recorded in CDCl_3 . The peaks obtained were consistent with the structures of the synthesized compounds. The imino proton, for (1), was observed at 8.75 ppm, while in the reduced form, the singlet at δ 3.92, due to $-\text{CH}_2$ -group, confirms the formation of the reduced Schiff base. The ^{13}C NMR spectrum showed the signals due the methyl carbon at 48.7 ppm, and the peaks which appeared in the range 120.56–151.52 ppm reflect the aromatic carbons. The signal due to the imino carbon, in (1), appeared at 161.56 ppm.

3.2. Corrosion measurement

3.2.1. OCP measurements

The magnitude of the OCP for samples can be a precise indication of their electrochemical activity. It is found that carbon steel with a lower OCP value will dissolve faster than the electrode with a higher OCP value in a solution with fixed oxidation-reduction potential (ORP) [56]. The OCP evolution of the carbon steel in 1.0 M HCl solution in the absence and presence of different concentrations of inhibitors (1) and (2) is shown in Fig. 1. The OCP of carbon steel generally reached a steady-state condition in the first 300 s after being immersed in the test solutions. As depicted in Fig. 1a, the OCP of carbon steel in solutions containing (1) shows a higher value than the (1)-free solution, indicating a higher inhibition activity. Furthermore, the OCP value gradually increases from -456 to -428 mV vs. Ag/AgCl on increasing the inhibitor (1) concentration in the range of 0.2 – 2.0 mM. These results confirm that a higher concentration of (1) promotes the inhibition efficiency of samples in a 1.0 M HCl solution. It is clear that OCP of carbon steel in the (2) containing solutions is in the potential range of -435 to -422 mV vs. Ag/AgCl, which shows a narrow potential range compared to (1)-containing solutions. Like the result of the (1), a 1.0 M HCl solution containing (2) has a higher OCP compared to the (2)-free solution. It can be concluded that the electrochemical activity of carbon steel electrodes in 1.0 M HCl containing (2) is lower than that in (2)-free solution. It can be inferred from Fig. 1b that the electrochemical activities for (2)-containing solutions follows the sequence: $0.2 \text{ mM} \geq 1.0 \text{ mM} > 2.0 \text{ mM}$. On the other hand, carbon steel electrodes in 2.0 mM (1)-containing solution showed the highest OCP values, which resulted in the highest corrosion resistance compared to lower concentrations. Overall, the OCP range of carbon steel in (2)-containing solutions is higher than (1)-containing solutions.

3.2.2. Potentiodynamic polarization

A Tafel diagram, as presented in Fig. 2, can be used to determine electrochemical parameters, including the corrosion current density, i_{corr} , equilibrium potential of carbon steel, and corrosion rate. Additionally, the cathodic coefficients (β_c) and the apparent anodic coefficients (β_a) are calculated by the aid of slopes of the Tafel diagram and

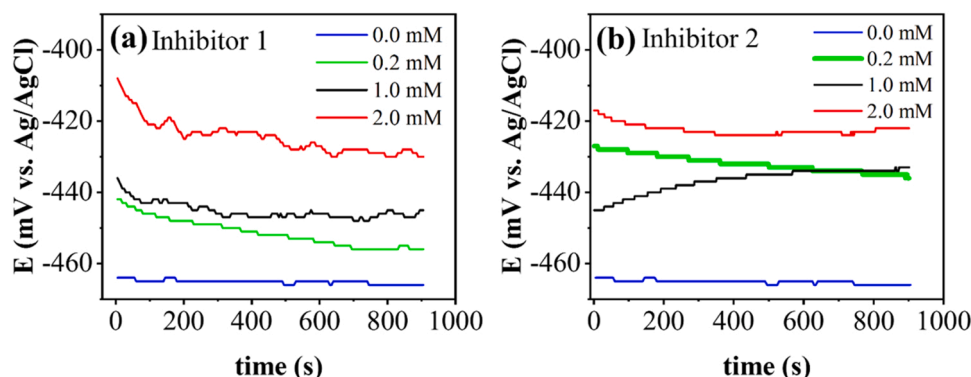


Fig. 1. The OCP value of carbon steel in 1.0 M HCl at different concentrations of (a) 1 and (b) 2.

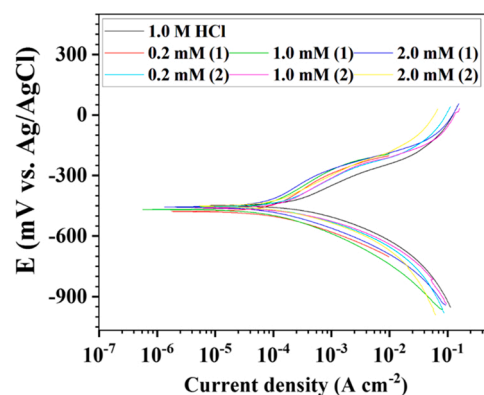


Fig. 2. Tafel diagram for carbon steel in 1.0 M HCl solution in the absence and various concentration inhibitors of (1) and (2).

Tafel equations, as follows:

$$\log i_{\text{ox}} = \log i + \frac{\alpha_a n F \eta}{2.3 RT} \quad (3)$$

$$\log i_{\text{red}} = \log i - \frac{\alpha_c n F \eta}{2.3 RT} \quad (4)$$

Where i_{red} and i_{ox} are the reduction and oxidation current densities, n , F , T , R demonstrates the number of transferred electrons, faradaic constant, absolute temperature (K), and ideal gas constant, respectively. The Tafel curves of the carbon steel in the absence and presence of inhibitors revealed similar polarization diagrams, implying no considerable difference in the polarization result between the inhibitor-free and inhibitor-containing solutions.

The i_{corr} for carbon steel is a precise measurement of its corrosion damage. As a result, an electrode with a higher i_{corr} will corrode faster than that with a lower i_{corr} at fixed oxidation-reduction potential (ORP) [57,58]. For the corrosion measurement of the present study, the values of standard deviation for two parallel electrochemical experiments are lower than 3.5%, indicating relatively excellent reproducibility of the corrosion determination. By assessing Table 2 data, the i_{corr} of carbon steel electrode in 1.0 M HCl solution is $2.33 \times 10^{-4} \text{ A/cm}^2$ representing the highest value among the other inhibitor-containing solutions. The i_{corr} for carbon steel in (1)-containing solution decreases gradually from 1.86×10^{-4} to $1.30 \times 10^{-4} \text{ A/cm}^2$ by raising the concentration of (1) from 0.2 to 2.0 mM. It is seen that the addition of the reduced form of (1) in the 1.0 M HCl solution provided a superior result with the best resistance to corrosion as compared to (1)-free and (1)-containing solutions. Along with the increase in the concentration of (2) from 0.2 to 2.0 mM, the i_{corr} is reduced by about 28%. A similar conclusion can be drawn by using results of the corrosion rate, in which carbon steel showed a higher corrosion resistance in (2)-containing solution in

Table 2

Tafel diagram data for carbon steel in 1.0 M HCl solution in the absence and various concentration inhibitors of (1) and (2).

Sample	Conc. (mM)	E_{corr} (mV)	i_{corr} (A/cm^2)	Corrosion rate (mm/year)	β_a (V/dec)	$-\beta_c$ (V/dec)	$-\beta_a/\beta_c$
1.0 M HCl (1)	0	-468.80	2.33×10^{-4}	2.71	0.111	0.123	0.90
	0.2	-463.40	1.86×10^{-4}	2.19	0.149	0.105	1.41
	1.0	-457.81	1.13×10^{-4}	1.51	0.169	0.150	1.13
	2.0	-455.30	1.30×10^{-4}	1.36	0.153	0.140	1.09
(2)	0.2	-455.39	1.40×10^{-4}	1.87	0.145	0.133	1.10
	1.0	-452.71	1.01×10^{-4}	1.18	0.154	0.141	1.09
	2.0	-451.58	1.00×10^{-4}	1.16	0.137	0.128	1.07

comparison to a 1.0 M HCl and (1)-containing solutions. Based on Table 2 data, the trend in corrosion inhibition efficiency measured from R_{ct} values of inhibitors is that inhibitor (2) > inhibitor (1). Haque et al. [37] have reported that the corrosion protection of steel in 1.0 M HCl enhances with increase in the concentration of chitosan Schiff bases (CSBs) in the range of 0–50 ppm. The corrosion current densities for the samples in inhibitor-containing solution which are reported in their work were in the range of 2.67–95.3 ($\times 10^4 \text{ A}/\text{cm}^2$). As compared with our results, the i_{corr} for the carbon steel in the presence inhibitors (1) and (2) solution are lower than that reported in their work [37]. The positive shifts in E_{corr} has been observed by increasing the concentration of both inhibitors (1) and (2) (Table 2). The results confirm that the change in E_{corr} detected by variation of the type of inhibitors and concentrations in the range of 0–2.0 mM, was evidence of rearrangement of cations and anions on the electrode surface. The shifts in the E_{corr} for the samples in inhibitors (1) and (2)-containing were 13 and 17 mV rather than inhibitor-free solution, indicating a mixed-type inhibition affect with predominant anodic effect in the corrosion behaviour of carbon steel in inhibitor-containing 1.0 M HCl [59]. The same trend has been reported for protected mild steel in 1.0 M HCl in the presence of PPQ and MPPQ inhibitors [23].

From Table 2, in all the solutions (except inhibitor-free solution) β_a is greater than β_c , indicating that the double layer formed on the surface of the carbon steel electrode shows the p-type semiconductor behavior [56]. Generally, both apparent charge transfer coefficients decrease by increasing the concentration of inhibitors. In addition, it is observed that

the reduced form of the inhibitor has hydrolytically a higher stability in hydrochloric acid media, owing to the fact that the reduced amine, where the imine ($-\text{C}=\text{N}-$) group is converted to an amine ($-\text{C}-\text{NH}-$) group [60], does not undergo hydrolysis [12,20].

3.2.3. EIS study

The simulated and measured Nyquist impedance spectra of carbon steel at the OCP in the absence and presence of inhibitors, (1) and (2), are shown in Fig. 3a and b. Only one time constant can be seen in the testing frequency range for the samples in 1.0 M HCl both with and without inhibitors, which is generally attributed to a process that mainly corresponds to a charge transfer phenomenon on the electrode surface. All Nyquist impedance spectra show a similar capacitive and a single loop, indicating that the corrosion mechanism is the same in inhibitor-free and containing solutions and moreover, the corrosion on the carbon steel is controlled by charge transfer process [54,61,62]. The Nyquist diagram obtained in different concentrations of (1) and its reduced form attributed to the capacitive impedance of a double-layer electrode. It is worth mentioning that the shape of Nyquist diagrams is a depressed semi-circle and accommodates the non-ideal behavior of a capacitance. This phenomenon illustrates using constant phase element (CPE), which includes two electrochemical parameters; Y_0 (the admittance of CPE) and n (empirical constant). The value of less than 1.0 arises from the roughness of the carbon steel surface and inhomogeneity owing to the adsorption of inhibitors together with the products of the

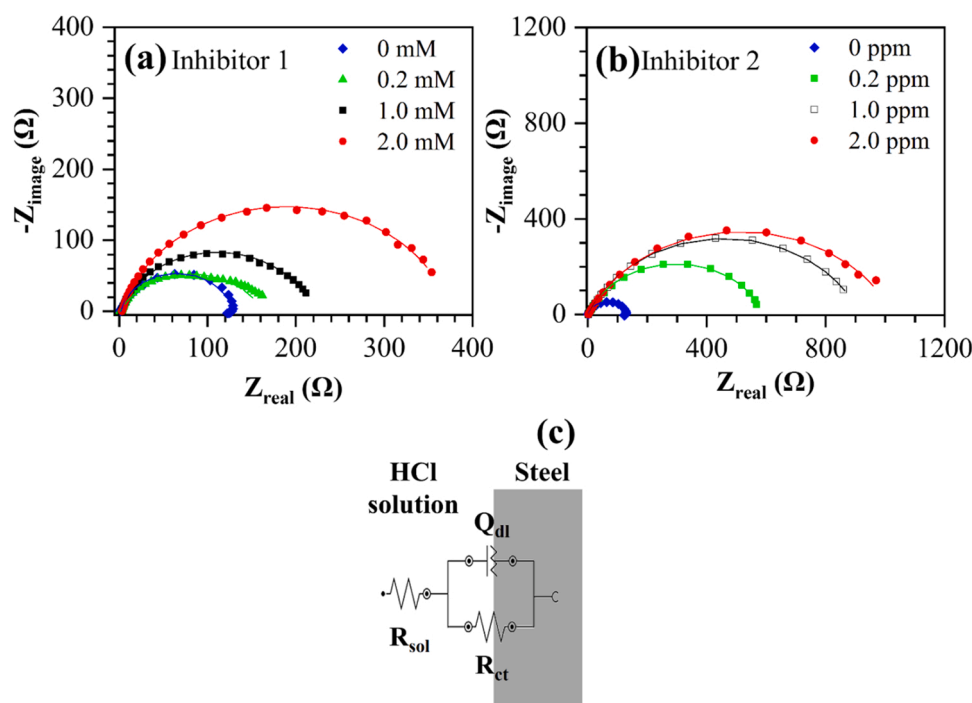


Fig. 3. Simulated and measured Nyquist impedance spectra of carbon steel at OCP 1.0 M HCl at different concentrations of (a) (1) and (b) (2), and (c) an equivalent circuit on the electrode surface.

corrosion process [63]. The equivalent electrical circuit is depicted in Fig. 3c, and its electrochemical parameters are shown in Table 3. An equivalent electrical circuit designed to fit EIS diagrams contains a resistance of 1.0 M HCl solution (R_{sol}) in series with Q_{dl}/R_{ct} .

As already known, charge transfer resistance is a characteristic quantity for corrosion resistance, as the higher the charge transfer resistance, the higher the corrosion resistance. From charge transfer resistance values given in Table 3, the resistance obtained in the presence of (1) was quite higher than that in the absence of (1) ($126.06 \Omega \text{ cm}^2$). Also, the trend for efficiency of inhibition for (1) follows the order of $2.0 \text{ mM} > 1.0 \text{ mM} > 0.2 \text{ mM}$. The charge transfer resistance for carbon steel in (1)-containing solution increases significantly from 170.0 to $371.6 \Omega \text{ cm}^2$ by increasing the concentration of (1) from 0.2 to 2.0 mM . The increment in charge transfer resistance at higher concentration is due to the fact that more inhibitor can be adsorbed on the carbon steel, so that the performance of corrosion inhibition would undoubtedly improve. It is apparent in Table 3 that on increasing the (2) concentration, an enormous increase in the value of R_{ct} is observed (588.8 – $1084.0 \Omega \text{ cm}^2$). As a result, the EIS data for inhibitors confirms that (2)-containing solutions have much better corrosion resistance for carbon steel than that for compound (1). These results are in good agreement with the Tafel experiments. In addition, many researchers have observed an increase in R_{ct} with a rise in the concentration of inhibitors, indicating higher inhibition efficiency at higher concentrations [23,28–30].

Generally, an increase in inhibitor concentration leads to an increment in the thickness and surface coverage of adsorbed molecules in the inhibitor layer, which are effectively adsorbed on the electrode surface [54]. On the other hand, the inhibitor molecules replace water, hydrogen and chloride ions adsorbed on the carbon steel surface [64]. Based on the FTIR results, the other reason for this phenomenon can be their inherent feature that N-containing functional groups play as an electron donor to the electrode surface [7,39]. The existence of hetero elements and aromatic rings such as nitrogen and sulfur on the structure of amino acids causes a substantial increase in inhibition efficiency [65].

The lower capacitance of the double-layer can be evidence of the higher efficiency of the inhibitor performance. The value of the double layer capacitance is calculated by the following equation:

$$C_{dl} = \left(\frac{Y_0}{R_{ct}^{n-1}} \right)^{\frac{1}{n}} \quad (5)$$

where C_{dl} is capacitive of double layer, Y_0 represents the value of CPE, R_{ct} is the charge transfer resistance and, n is the phase exponent, which is always in the range of 0 – 1 . As the following equation, C_{dl} is inversely related to the thickness of the double layer, which serves as a barrier layer for protection from corrosion.

$$C_{dl} = \frac{\epsilon \epsilon_0 A}{d} \quad (6)$$

where d is the thickness of the electrical double layer, ϵ_0 is vacuum permittivity, ϵ is dielectric constant, and A is the electrode area in the electrolyte. In contrast with R_{ct} , the capacitance of double layer (C_{dl})

show a reverse dependence on the concentration of inhibitor: more inhibitor gives rise to lower C_{dl} (Fig. 4). An increase in (1) concentration leads to a gradual decrease in the value of C_{dl} (42.10 – $34.85 \mu\text{F cm}^{-2}$), which implies a reduction in local dielectric constant or/and increase in the double layer thickness [63]. The C_{dl} for carbon steel in (2) containing solutions decreases from 38.84 to $23.56 \mu\text{F cm}^{-2}$ by increasing the inhibitor concentration, which demonstrates lower C_{dl} values than (1)-containing solutions. Along with this outcome, it has been previously reported that the more decrease in the capacitance value of carbon steel is, the more concentration of the inhibitor is [22,29,30,39].

Therefore, carbon-steel shows higher corrosion resistance in (2)-containing solutions compared to (1)-containing solutions. This phenomenon reflects that the presence of inhibitors (1) and (2) have led to the decrement in capacitance of the double layer due to the replacement of H_2O molecules by inhibitor ions at the surface of the carbon steel electrode [39]. As a result of the adsorption of inhibitors on the electrode surface, the effective value of area (A), which can intensify the rate of corrosion, decreased, and the efficiency of surface protection is increased. The adsorption of molecules of (1) and (2) on the electrode surface acts as a barrier for ions and charge transfers between metal and electrolyte, thus enhances the protecting surface from corrosion. These findings confirm the data obtained in EIS analysis, in which higher charge transfer resistance led to higher protection efficiency. By assessing the obtained in EIS measurements, it is fair to say that the reduction of inhibitor has improved the inhibition efficiency and the corrosion resistance of carbon steel in 1.0 M HCl solution. Furthermore, the inhibition mechanism has been confirmed by both measurements of EIS and Tafel.

Fig. 5 depicts the inhibition efficiency (IE) calculated from charge transfer resistance values obtained in EIS diagrams shown in Fig. 3 as follows:

$$IE(\%) = \frac{R_{ct} - R_{ct}^0}{R_{ct}} \times 100 \quad (7)$$

where R_{ct} and R_{ct}^0 present the charge transfer resistance of carbon steel

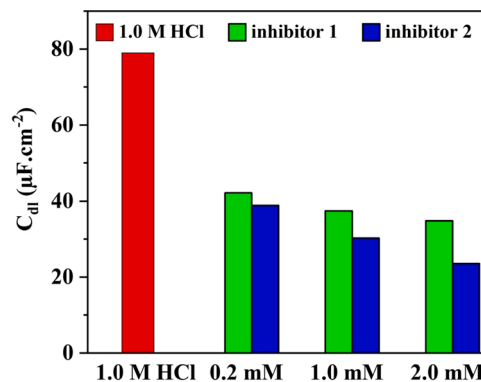


Fig. 4. The capacitance of double layer values of carbon steel in 1.0 M HCl solution containing different concentrations of inhibitors.

Table 3
EIS parameters for an equivalent circuit of Fig. 3c.

Inhibitor type	Concentration (mM)	R_{sol} ($\Omega \text{ cm}^2$)	R_{ct} ($\Omega \text{ cm}^2$)	Q_{dl}		χ^2
				Y_0 ($\Omega \text{ s}^{-n}$)	n	
1.0 M HCl (1)	0.0	2.41	126.06	1.31×10^{-4}	0.89	0.013
	0.2	7.80	170.00	9.75×10^{-5}	0.83	0.042
	1.0	2.63	216.50	9.35×10^{-5}	0.81	0.008
	2.0	3.39	371.60	6.69×10^{-5}	0.85	0.007
(2)	0.2	3.25	588.80	8.27×10^{-5}	0.80	0.011
	1.0	2.57	1024.0	6.96×10^{-5}	0.76	0.016
	2.0	5.06	1084.0	5.28×10^{-5}	0.78	0.035

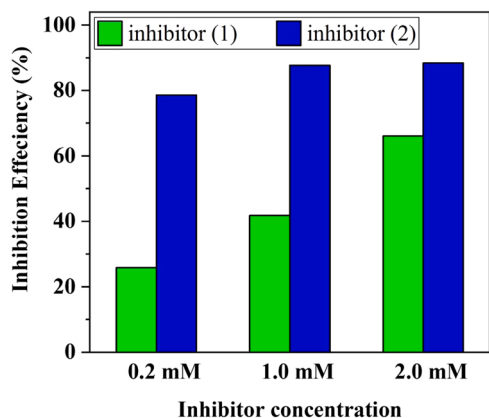


Fig. 5. The inhibition efficiency values of carbon steel in 1.0 M HCl solution containing different concentrations of inhibitors.

with and without inhibitors, respectively. The IE increased by adding more (1)-inhibitor with a maximum IE of 88.51% at 2.0 mM concentration. As can be seen in Fig. 5, there is a gradual increment in the efficiency of inhibition of (1)-containing solution from 25.84% to 66.08%, which represents a 60.9% improvement in corrosion protection by increasing inhibitor concentration from 0.2 mM to 2 mM (tenfold increase in inhibitor concentration). As the data shows in Fig. 5, the IE obtained in the presence of (2) is much greater than the values obtained in the presence of (1).

3.2.4. Immersion Tests

EIS technique provides a convenient and rapid way to follow the inhibiting performance over time. It is a reliable technique to characterize the surface layer owing not to disturb the interface of the metal

and the solution [66]. For this reason, the EIS measurements in inhibitor-free and inhibitor-containing 1.0 M HCl solution, up to 24 h immersion (1, 4 and 24 h) and at a concentration of 2.0 mM inhibitor (1) and (2) (optimum concentration) is shown in Fig. 6. From the Nyquist spectra it can be seen that when the carbon steel immersed into the solution for different times, the shape of the impedance spectra showed a semicircle and did not change considerably. This indicates that the electrochemical process on the electrode/solution interface is generally controlled by a charge transfer process. Whereas, the size of semicircle changes by prolonging the immersion in the solutions. The calculated charge transfer and inhibition efficiency (IE) variations with time are illustrated in Table 4. In the inhibitor-free solution, the values of R_{ct} showed a decrease with time. When the immersion time increased from 1 to 4 h, R_{ct} values demonstrate a slight decrement from 303.1 $\Omega\text{ cm}^2$ for uninhibited carbon steel to 298.3 $\Omega\text{ cm}^2$ after its 4 h exposure, showing some corrosion process take place. While, the value of R_{ct} decreases drastically from 298.3 to 4.6 $\Omega\text{ cm}^2$ after 24 h immersion into 1.0 M HCl, indicating the pitting corrosion occurred [67]. In addition, the higher value of R_{ct} in shorter immersion times (i.e. 1 and 4 h) can be related to the formation of an oxide/hydroxide iron layer on the carbon steel surface, which can reduce corrosion in acidic media [68].

Table 4

The calculated values of charge transfer resistance and IE of carbon steel in 1.0 M HCl inhibitor free and inhibitor-containing solution at different immersion time.

Immersion time (h)	1.0 M HCl	2.0 mM inhibitor 1	2.0 mM inhibitor 2		
	R_{ct} ($\Omega\text{ cm}^2$)	R_{ct} ($\Omega\text{ cm}^2$)	IE (%)	R_{ct} ($\Omega\text{ cm}^2$)	IE (%)
1	303.1	348.0	12.9	1055.2	71.3
4	298.3	503.9	40.6	1346.5	77.8
24	4.6	987.0	99.5	1521.5	99.7

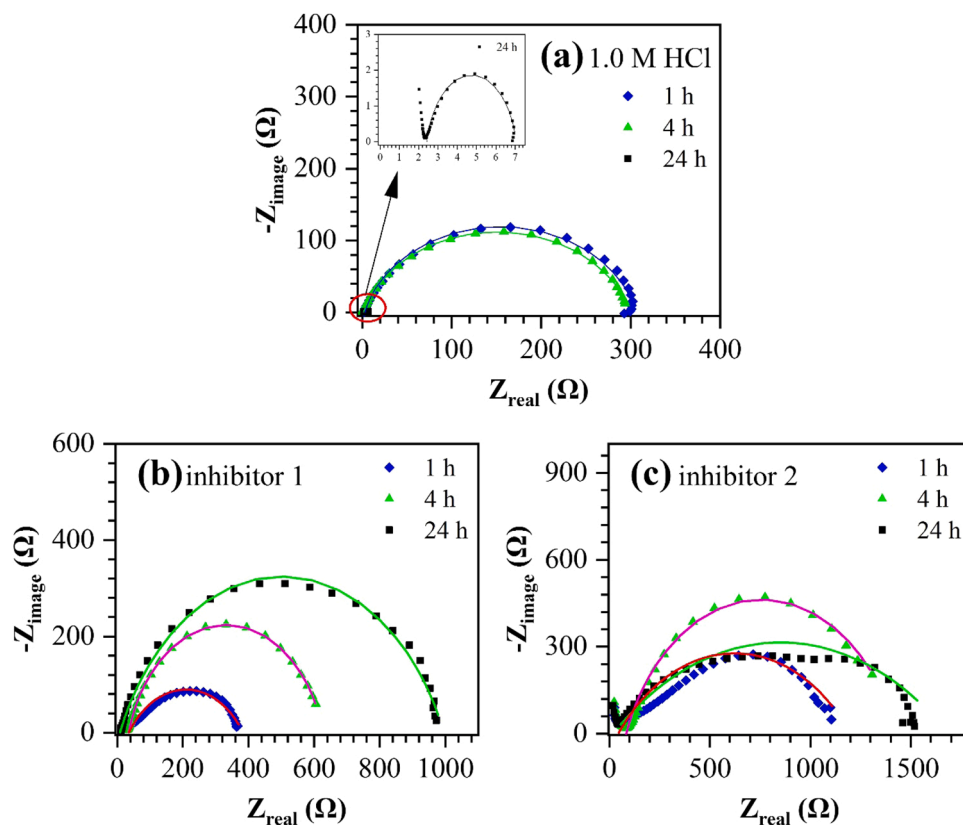


Fig. 6. Simulated and measured Nyquist impedance spectra of carbon steel at OCP 1.0 M HCl at different immersion times: 1, 4 and 24 h of (a) 1.0 M HCl and (b) inhibitor (1), and (c) inhibitor (2).

On the other hand, in the presence of inhibitors (1) and (2), the R_{ct} values are larger than that uninhibited solution. This phenomenon demonstrates the formation of a protective and compact thin layer of inhibitor molecules on the carbon steel surface. The general increasing in inhibiting efficiency with time is clearly revealed. The determined charge transfer resistance in 1.0 M HCl with inhibitor (1) was $348 \Omega \text{ cm}^2$ after a 1 h exposure. R_{ct} increased drastically $987.0 \Omega \text{ cm}^2$ at 24 h immersion in the inhibitor (1)-containing solution. This verified that when the exposure time was rising from 1 to 24 h, the inhibitor (1) molecules in the solution adsorb on the carbon steel surface and rearrange to form a compact and denser film gradually. Obviously, with the increasing immersion time, more inhibitor (1) and its derivative molecules in the solution were adsorbed on the metal surface, as a consequence the inhibiting performance became stronger [69]. Furthermore, compared the results of inhibitor (1) and (2), the IE improved remarkably by using (2), and the IE reached the maximum value of 99.7% after 24 h immersion of carbon steel in inhibitor (2)-containing solution. The diameter of the semicircle in the presence of the inhibitor (2) increased remarkably in comparison with 1 and 4 h exposure times. As a result, this indicated the continuous adsorption of inhibitor (2) on the metal surface and the approach in the improvement of surface protection.

3.3. Surface characterization

Fig. 6 demonstrates the SEM images and their EDS analysis of carbon steel surfaces before and after immersion in 1.0 M HCl in the absence and presence of inhibitors (1) and (2). As can be seen in Fig. 6a, the surface of the carbon steel before immersion in 1.0 M HCl is very smooth and clear and there is no corrosion on the surface. The EDS analysis of as-received carbon steel shows iron and carbon peaks corresponding to its natural composition. The sample immersed in inhibitor-free hydrochloric acid solution showed that the surface was severely corroded due to steel dissolution and aggressive ion attack (Fig. 6b). It has been reported that the surface of steel sample became seriously corroded in a free-inhibitor 1.0 M HCl [23]. The presence of an oxygen peak in the EDS spectrum of the carbon steel exposed to 1.0 M HCl in the absence of inhibitors signifies the formation of the oxide products due to the steel corrosion. In contrast, the surfaces of the carbon steel in the presence of 2.0 mM (1) and (2) are much less corroded than the sample immersed in 1.0 M HCl (Fig. 6c and d) indicating that substantial protection to the carbon steel surface is provided by the synthetic inhibitors. It is notable that the inhibitor (2) showed better performance in comparison to inhibitor (1), which was confirmed by there being no considerable variation of the surface, except for the emery lines. The lack of presence of oxygen peak in the carbon steel sample immersed in 1.0 M HCl containing inhibitor (2) confirms again that obtained results. Generally, the presence of synthetic inhibitors reduced the steel atoms participating in corrosion reaction and consequently increases the lifetime of samples in aggressive acidic solutions. The smooth surface for carbon steel in inhibitor-containing solution (e.g. PPQ and MPPQ) has been observed by Chen et al. [23]. They reported that the corrosion of steel greatly reduced with PPQ and MPPQ by a protective film formation on the metal surface. Amini et al. [21] has been reported that the surface of mild steel dipped in the chloride solution for 24 h can be protected by adding inhibitor. It is fair that our observation of the protected surface of steel are quite similar or better than the other research works on this area [21, 23].

Based on the obtained results in EIS analysis, the charge transfer resistance for 1.0 M HCl was equal $126.06 \Omega \text{ cm}^2$, which was lower than the all samples in inhibitor-containing solutions. As compared with SEM image of steel surface in 1.0 M HCl (Fig. 6a), horrible and fearful corrosion of sample took place by attack from strong acidity and chloride ions. This observation is fairly accordance with EIS findings, in which the sample in inhibitor-free solution did not suffer aggressive attack from chloride solution. While, corrosion resistance improvement was detected with both inhibitor (1) and (2) (e.g. Fig. 6c and d). As the

best corrosion resistance, charge transfer resistance, as high as $1084.0 \Omega \text{ cm}^2$, was achieved with inhibitor (2)-containing solution for carbon steel. As can be seen in Fig. 6d, the SEM image of the carbon steel is obviously similar to the as-received carbon steel one (Fig. 6a). The carbon steel surface in a 2 mM inhibitor (2) solution looks more smooth and uniform than the corroded one in the inhibitor-free solution (Fig. 6b). Based on the EIS results, the relatively poor protection from chloride ions for the samples in inhibitor (1) compared inhibitor (2) is clearly consistent with our observation in the SEM images (e.g. Fig. 6c and d). Therefore, the inhibitor protection from the corrosive 1.0 M HCl solution can be confirmed by the SEM image and EIS analysis of the carbon steel samples.

3.4. Adsorption and inhibition mechanism

The adsorption of inhibitor on the surface of the carbon steel electrode is a vital step in an inhibition mechanism [70]. The main reason for higher corrosion protection in the presence of inhibitors is the adsorption of this material on the carbon steel surface. The cathodic corrosion reaction is hydrogen evaluation on the surface of carbon steel, which is accomplished by the following pathway [39]:



The adsorption of inhibitor molecules can occur on the carbon steel instead of the hydrogen ions at the cathodic region. Therefore, the rate of hydrogen molecules evaluation can decrease effectively [66]. In the inhibitor-free 1.0 M HCl solutions, the following anodic reactions is proposed at the anodic sites:



According to above mechanisms, $(FeCl^-)_{ads}$ groups formed on the carbon steel surface through the reaction (11) by the adsorption of the chloride ions. This group undergoes two-electron loss by the reactions (12) and (13) to form cationic iron chloride on the metal surface. At the final stage, corrosion reaction of carbon steel occurs by the decomposition process (reaction (14)). While, in terms of the inhibitor-containing solution, nitrogen molecules in imine group can be able to protonate and adsorb at the anodic sites on the carbon steel surface by electrostatic bond with $(FeCl^-)_{ads}$ species [39]. The following reaction can take place in competition with the chloride ions adsorption on the metal surface:



Thereby, in the case of inhibitor containing solutions, the rate of reaction (15) should be much faster than electron-loss reactions, as it can be confirmed by the lower values of absolute adsorption free energy, calculating by the adsorption model.

Based on the previous studies [12,54], the Langmuir adsorption model is the best model to explain the adsorption process of the inhibitors on the surface of carbon steel in 1.0 M HCl. The Langmuir relationship, a plot of C/θ against C , should yield a straight line with a slope of unity for inhibitor-containing solutions. Based on the calculations, the slopes of the lines obtained 1.47 for (1) and 1.22 for (2), which are far from being equal to one, suggesting that they do not follow the Langmuir adsorption model. In addition, the outcome of the Langmuir isotherm reveals that the correlation regression coefficient (R^2) values

for inhibitors are found to be 0.841 and 0.892, again it confirm that the inhibitor (1) and (2) adsorption on steel surface do not follow the Langmuir monolayer adsorption.

The data were plotted as the Temkin isotherm (Fig. 7), a model that gives a good fitting to the experimental data. The Temkin adsorption isotherm is presented as follows:

$$\exp(-2a\theta) = KC_{inh} \quad (16)$$

where c is the inhibitor concentration, a is an interaction parameter, and K the adsorption coefficient and θ the fraction of surface coverage by the inhibitor molecules, which the calculation formula of θ was as follows [38]:

$$\theta = 1 - \frac{C_{dl}^i}{C_{dl}^b} \quad (17)$$

where C_{dl}^b and C_{dl}^i are the capacitive response of the carbon steel electrode in a free-inhibitor and containing inhibitor solution. Temkin adsorption isotherm, a plot of $\ln(C_{inh})$ against θ , is shown in Fig. 7. The R^2 values (shown in Fig. 7) give a good agreement between the EIS and Temkin data for inhibitor (1) ($R^2 = 0.0.9401$) and inhibitor (2) ($R^2 = 0.9720$). The values of a and K are -12.13 and 3.36×10^5 for (1) and -6.08 and 2.12×10^3 for (2). The negative values of a indicate repulsion forces among the surface adsorbed molecules [71]. It has been observed that value in (1) and (2)-containing solution is negative, revealing that repulsive force exists in the adsorption surface. It is well known that the value of K illustrates the strength between the adsorbent and adsorbate [72]. The higher values of K , the better inhibition efficiency will give in 1.0 M HCl [71]. According to K values, the reduced form of (1) shows higher strength among the adsorbate and steel surface

than (1)-containing solution.

3.5. Theoretical studies

Theoretical calculations are a widely used method that provides important information about many properties of molecules and for this study the Gaussian software program was used. In this program, many quantum chemical parameters were obtained using the basis sets of the B3lyp, HF, and M062X method 6-31 + +G(d,p). The resulting values of these parameters are given in Table 4 and Table 5. The two most important and most commonly used parameters among those obtained are the numerical values of the HOMO (Highest Occupied Molecular Orbital) and LUMO (Lowest Unoccupied Molecular Orbital) of the inhibitor molecules.

The HOMO energy values of the inhibitor molecules show the ability of inhibitor molecules to donate electrons. The LUMO energy value shows the inhibitor molecules' ability to receive electrons. These two parameters are used to explain the ability of inhibitor molecules to become inhibitors to prevent corrosion by binding with metal atoms. The molecule with the highest HOMO energy value of the inhibitor molecules has the highest inhibitory activity [73]. On the other hand, the inhibitor molecules with the lowest LUMO energy value have the highest inhibitory activity [74]. Another important parameter is GAP, which refers to the difference between the energy values of the HOMO and LUMO orbitals; the molecule with the lowest numerical value of this parameter has the highest inhibitory activity, because a low value of this parameter facilitates electron transfer [75].

Fig. 8 shows the optimized structures of the inhibitor molecules (1) and (2) as well as the HOMO, LUMO, and ESP representations. Many quantum chemical parameters of molecules have been calculated by

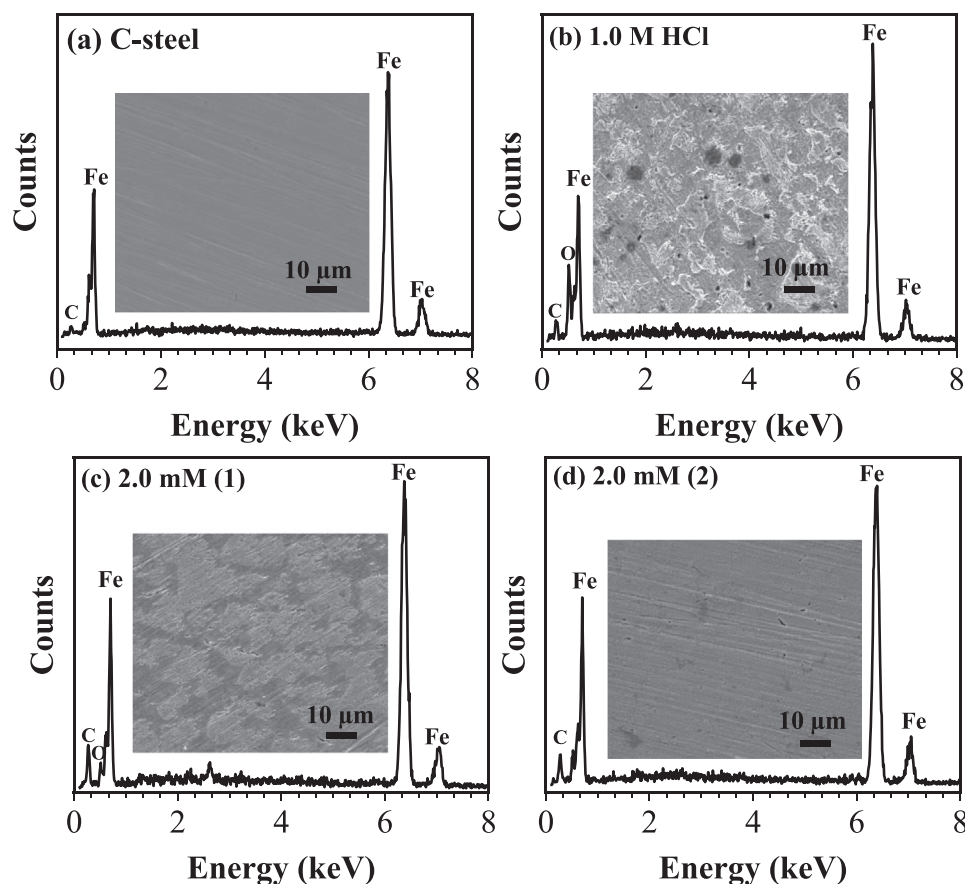


Fig. 7. (a) SEM image and EDS analysis of the as-received carbon steel surface, and SEM image of carbon steel taken after immersion in (b) 1.0 M HCl (inhibitor-free), (c) 2.0 mM inhibitor (1) and (d) 2.0 mM inhibitor (2).

Table 5

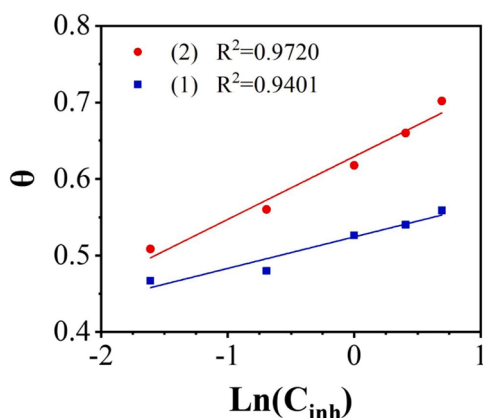
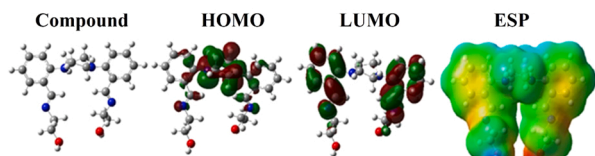
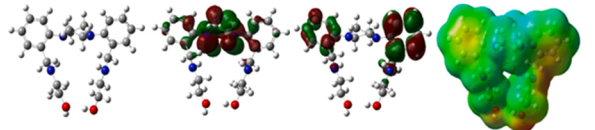
The calculated quantum chemical parameters of molecules.

	E_{HOMO}	E_{LUMO}	I	A	ΔE	η	σ	χ	Pi	ω	ε	dipol	Energy
B3LYP /6–31 g LEVEL													
X1	-5.7504	-1.4939	5.7504	1.4939	4.2564	2.1282	0.4699	3.6221	-3.6221	3.0824	0.3244	2.0622	-33313.9859
X2	-5.5229	-0.5546	5.5229	0.5546	4.9683	2.4841	0.4026	3.0387	-3.0387	1.8585	0.5381	0.1660	-33378.6669
HF/6–31 g LEVEL													
X1	-8.8081	0.9543	8.8081	-0.9543	9.7624	4.8812	0.2049	3.9269	-3.9269	1.5796	0.6331	4.0602	-33102.5069
X2	-8.8370	0.9685	8.8370	-0.9680	9.8054	4.9027	0.2040	3.9343	-3.9343	1.5785	0.6335	4.6558	-33164.7402
M062X/6–31 g LEVEL													
X1	-6.7354	-0.2314	6.7354	0.2314	6.5040	3.2520	0.3075	3.4834	-3.4834	1.8656	0.5360	1.6045	-33360.2485
X2	-6.7849	-0.2411	6.7849	0.2411	6.5438	3.2719	0.3056	3.5130	-3.5130	1.8859	0.5302	1.6849	-33363.6069

Table 6

The calculated quantum chemical parameters of protonated form.

	E_{HOMO}	E_{LUMO}	I	A	ΔE	η	σ	χ	Pi	ω	ε	dipol	Energy
B3LYP /6–31 g LEVEL													
X1	-8.0476	-4.3656	8.0476	4.3656	3.6820	1.8410	0.5432	6.2066	-6.2066	10.4621	0.0956	11.6628	-33323.4206
X2	-7.7703	-4.3988	7.7703	4.3988	3.3715	1.6858	0.5932	6.0845	-6.0845	10.9806	0.0911	14.7274	-33387.9930
HF/6–31 g LEVEL													
X1	-10.8068	-2.0153	10.8068	2.0153	8.7915	4.3958	0.2275	6.4111	-6.4111	4.6751	0.2139	12.5751	-33111.8134
X2	-10.7842	-2.3187	10.7842	2.3187	8.4655	4.2328	0.2363	6.5515	-6.5515	5.0702	0.1972	16.2184	-33173.9645
M062X/6–31 g LEVEL													
X1	-9.4721	-3.7288	9.4721	3.7288	5.7433	2.8716	0.3482	6.6004	-6.6004	7.5855	0.1318	12.0291	-33308.7439
X2	-10.7842	-2.3187	10.7842	2.3187	8.4655	4.2328	0.2363	6.5515	-6.5515	5.0702	0.1972	16.2185	-33173.9643

**Fig. 8.** Temkin adsorption isotherms involving inhibitor (1) and its reduced form (2).**(a) Inhibitor (1)****(b) Inhibitor (2)****Fig. 9.** Representations of optimized structures, HOMO, LUMO, and ESP shapes of (a) inhibitor (1) and (b) inhibitor (2) molecules.

theoretical calculations. The most important of these calculated

parameters are HOMO and LUMO. When the numerical value of the HOMO parameter is compared, it is generally seen that the numerical value of the HOMO parameter of compound 2 is more negative at the M062X/6–31 g level. Therefore, it is seen that the inhibitory activity of (1) is higher. On the other hand, when the numerical value of the LUMO parameter of the molecules is examined, it is seen that the LUMO energy value of (2) is more positive at the M062X/6–31 g level. However, it is seen that the DE energy gap value is larger in (2) than in the other molecule. It is seen that the inhibitory activity of compound 1 with a small DE energy gap value is higher.

It was seen that the parameters obtained as a result of the calculations were in great agreement with the experimentally obtained data. The obtained parameters confirm that Compound 1 is a better corrosion inhibitor.

4. Conclusion

The corrosion behavior of carbon steel in 1.0 M HCl with and without inhibitors was investigated by using electrochemical techniques. From Tafel results, the i_{corr} for carbon steel in (1) and (2)-containing solution decreases by raising the concentration of (1) and (2) from 0.2 to 2.0 mM. The reduced form (2) was found to show a better inhibitor characteristic than (1) due to the higher stability in an HCl solution. An increment of inhibitor (1) and (2) concentration, while the charge transfer resistance of carbon steel enhanced as the inhibitor concentration increased. The result showed that the inhibition efficiency of (2) enhances with increasing the concentration and presented the highest value at a concentration of 2.0 mM (e.g., 88.37%). The SEM images and EDS analyses of the carbon steel in inhibitor free and containing solutions revealed that the surface of electrode is well protected by adsorption of inhibitor molecules on the metal surface, even after 12 hr immersion in corrosive solution. Adsorption of both inhibitors, (1) and its reduced form (2), was found to obey the Temkin adsorption isotherm. As a result of the quantum chemical parameters of the inhibitor molecules with theoretical calculations, it has been observed that the inhibitor (1) has more inhibitory activity than the other molecule. Since the made theoretical calculations are made in a pure and isolated environment, it is quite normal that there are differences between experimental procedures.

CRediT authorship contribution statement

Majid Rezaeivala: Conceptualization, Synthesis and characterization of inhibitors, Writing – review & editing. **Saeid karimi:** Data curation, Methodology, Writing – review & editing. **Burak Tuzun:** Software, Writing – review & editing. **Koray Sayin:** Software, Writing – review & editing, Investigation, Validation.

Declaration of Competing Interest

The authors declare that they have no known competing financial interests or personal relationships that could have appeared to influence the work reported in this paper.

Acknowledgment

We thank Hamedan University of Technology. Also, this work was supported by Research Fund of TÜBİTAK ULAKBİM High Performance and Grid Computing Center (TR-Grid e-Infrastructure). The authors would like to thank Dr. Robert W. Gable, University of Melbourne, for constructive criticism of the manuscript.

References

- [1] H. Jafari, K. Sayin, Sulfur containing compounds as corrosion inhibitors for mild steel in hydrochloric acid solution, *Trans. Indian Inst. Met.* 69 (2016) 805–815, <https://doi.org/10.1007/s12666-015-0556-2>.
- [2] M. Shabani-Nooshabadi, M.S. Ghandchi, Santolina chamaecyparissus extract as a natural source inhibitor for 304 stainless steel corrosion in 3.5% NaCl, *J. Ind. Eng. Chem.* 31 (2015) 231–237, <https://doi.org/10.1016/j.jiec.2015.06.028>.
- [3] A. Singh, K.R. Ansari, M.A. Quraishi, H. Lgaz, Effect of electron donating functional groups on corrosion inhibition of J55 steel in a sweet corrosive environment: experimental, density functional theory, and molecular dynamic simulation, *Materials* 12 (2018) 233–251, <https://doi.org/10.3390/ma12010017>.
- [4] F. Mohsenifar, H. Jafari, K. Sayin, Investigation of thermodynamic parameters for steel corrosion in acidic solution in the presence of N,N'-Bis(phloroacetophenone)-1,2 propanediamine, *J. Bio Tribo Corros.* 2 (2016) 1, <https://doi.org/10.1007/s40735-015-0031-y>.
- [5] K.M. Shainy, P. Rugmini Ammal, K.N. Unni, S. Benjamin, A. Joseph, Surface interaction and corrosion inhibition of mild steel in hydrochloric acid using pyoverdine, an eco-friendly bio-molecule, *J. BioTribo Corros.* 2 (2016) 1–12, <https://doi.org/10.1007/s40735-016-0050-3>.
- [6] L. Toukal, S. Keraghel, F. Benganem, A. Ourari, Electrochemical, thermodynamic and quantum chemical studies of synthesized benzimidazole derivative as an eco-friendly corrosion inhibitor for XC52 steel in hydrochloric acid, *Int. J. Electrochem. Sci.* 13 (2018) 951–974, <https://doi.org/10.20964/2018.01.43>.
- [7] R. Rihan, R. Shawabkeh, N. Al-Bakr, The effect of two amine-based corrosion inhibitors in improving the corrosion resistance of carbon steel in sea water, *J. Mater. Eng. Perform.* 23 (2014) 693–699, <https://doi.org/10.1007/s11665-013-0790-x>.
- [8] A.L. de, Q. Baddini, S.P. Cardoso, E. Hollauer, J.A. da, C.P. Gomes, Statistical analysis of a corrosion inhibitor family on three steel surfaces (duplex, super-13 and carbon) in hydrochloric acid solutions, *Electrochim. Acta* 53 (2007) 434–446, <https://doi.org/10.1016/j.electacta.2007.06.050>.
- [9] Z. Tang, A review of corrosion inhibitors for rust preventative fluids, *Curr. Opin. Solid State Mater. Sci.* 23 (2019), 100759, <https://doi.org/10.1016/j.cossms.2019.06.003>.
- [10] J. Haque, C. Verma, V. Srivastava, M.A. Quraishi, E.E. Ebenso, Experimental and quantum chemical studies of functionalized tetrahydropyridines as corrosion inhibitors for mild steel in 1 M hydrochloric acid, *Results Phys.* 9 (2018) 1481–1493, <https://doi.org/10.1016/j.rinp.2018.04.069>.
- [11] Y. El Aoufir, R. Aslam, F. Lazrak, R. Marzouki, S. Kaya, S. Skal, A. Ghanimi, I.H. Ali, A. Guenbour, H. Lgaz, I.M. Chung, The effect of the alkyl chain length on corrosion inhibition performances of 1,2,4-triazole-based compounds for mild steel in 1.0 M HCl: Insights from experimental and theoretical studies, *J. Mol. Liq.* 303 (2020), 112631, <https://doi.org/10.1016/j.molliq.2020.112631>.
- [12] A.B. da Silva, E. D'Elia, J.A. da Cunha Ponciano Gomes, Carbon steel corrosion inhibition in hydrochloric acid solution using a reduced Schiff base of ethylenediamine, *Corros. Sci.* 52 (2010) 788–793, <https://doi.org/10.1016/j.corsci.2009.10.038>.
- [13] I.B. Onyeachu, M.M. Solomon, Benzotriazole derivative as an effective corrosion inhibitor for low carbon steel in 1 M HCl and 1 M HCl + 3.5 wt% NaCl solutions, *J. Mol. Liq.* 313 (2020), 113536, <https://doi.org/10.1016/j.molliq.2020.113536>.
- [14] H. Rahmani, E.I. Meletis, Corrosion study of brazing Cu[sbnd]Ag alloy in the presence of benzotriazole inhibitor, *Appl. Surf. Sci.* 497 (2019), 143759, <https://doi.org/10.1016/j.apsusc.2019.143759>.
- [15] K. Sabet Bokati, C. Dehghanian, Adsorption behavior of 1H-benzotriazole corrosion inhibitor on aluminum alloy 1050, mild steel and copper in artificial seawater,

- [16] J. Environ. Chem. Eng. 6 (2018) 1613–1624, <https://doi.org/10.1016/j.jece.2018.02.015>.
- [17] J. Rodriguez, M. Mouanga, A. Roobroeck, D. Cossement, A. Mirisola, M.G. Olivier, Study of the inhibition ability of benzotriazole on the Zn-Mg coated steel corrosion in chloride electrolyte, *Corros. Sci.* 132 (2018) 56–67, <https://doi.org/10.1016/j.corsci.2017.12.025>.
- [18] G. Bahlakeh, M. Ramezanzadeh, B. Ramezanzadeh, Experimental and theoretical studies of the synergistic inhibition effects between the plant leaves extract (PLE) and zinc salt (ZS) in corrosion control of carbon steel in chloride solution, *J. Mol. Liq.* 248 (2017) 854–870, <https://doi.org/10.1016/j.molliq.2017.10.120>.
- [19] K.C. Emregül, O. Atakol, Corrosion inhibition of iron in 1 M HCl solution with Schiff base compounds and derivatives, *Mater. Chem. Phys.* 83 (2004) 373–379, <https://doi.org/10.1016/j.matchemphys.2003.11.008>.
- [20] K.M. Emran, N.M. Ahmed, B.A. Torjoman, A.A. Al-Ahmadi, S.N. Sheekh, Cantaloupe extracts as eco friendly corrosion inhibitors for aluminum in acidic and alkaline solutions, *J. Mater. Environ. Sci.* 5 (2014) 1940–1950.
- [21] E. Bartmatov, T. Hughes, Degradation of a schiff-base corrosion inhibitor by hydrolysis, and its effects on the inhibition efficiency for steel in hydrochloric acid, *Mater. Chem. Phys.* 257 (2021), 123758, <https://doi.org/10.1016/j.matchemphys.2020.123758>.
- [22] M. Amini, R. Naderi, M. Mahdavian, A. Badiei, Effect of piperazine functionalization of mesoporous silica type SBA-15 on the loading efficiency of 2-mercaptobenzothiazole corrosion inhibitor, *Ind. Eng. Chem. Res.* 59 (2020) 3394–3404, <https://doi.org/10.1021/acs.iecr.9b05261>.
- [23] I. Abdulazeez, Q. Peng, O.C.S. Al-Hamouz, M. Khaled, A.A. Al-Saadi, Evaluation of the inhibition performance of piperazine-based polyurea towards mild steel corrosion: the role of keto-enol tautomerization, *J. Mol. Struct.* 1248 (2022), 131485, <https://doi.org/10.1016/j.molstruc.2021.131485>.
- [24] W. Chen, B. Nie, M. Liu, H.J. Li, D.Y. Wang, W. Zhang, Y.C. Wu, Mitigation effect of quinazolin-4(3H)-one derivatives on the corrosion behaviour of mild steel in HCl, *Colloids Surf. A Physicochem. Eng. Asp.* 627 (2021), 127188, <https://doi.org/10.1016/j.colsurfa.2021.127188>.
- [25] A.O. Ayeni, O.F. Akinyele, E.C. Hosten, E.G. Fakola, J.T. Olalere, G.O. Egharevba, G.M. Watkins, Synthesis, crystal structure, experimental and theoretical studies of corrosion inhibition of 2-((4-(2-hydroxy-4-methylbenzyl)piperazin-1-yl)methyl)-5-methylphenol – a Mannich base, *J. Mol. Struct.* 1219 (2020), 128539, <https://doi.org/10.1016/j.molstruc.2020.128539>.
- [26] N.J.N. Nnaji, O.T. Ujam, N.E. Ibsi, J.U. Ani, T.O. Onuegbu, L.O. Olanunmi, E. E. Ebenso, Morpholine and piperazine based carboxamide derivatives as corrosion inhibitors of mild steel in HCl medium, *J. Mol. Liq.* 230 (2017) 652–661, <https://doi.org/10.1016/j.molliq.2017.01.075>.
- [27] Y. Li, H. Chen, B. Tan, B. Xiang, S. Zhang, W. Luo, Y. Zhang, J. Zhang, Three piperazine compounds as corrosion inhibitors for copper in 0.5 M sulfuric acid medium, *J. Taiwan Inst. Chem. Eng.* 126 (2021) 231–243, <https://doi.org/10.1016/j.jtice.2021.06.055>.
- [28] M. Rezaeivala, H. Keypour, Schiff base and non-Schiff base macrocyclic ligands and complexes incorporating the pyridine moiety – The first 50 years, *Coord. Chem. Rev.* 280 (2014) 203–253, <https://doi.org/10.1016/j.ccr.2014.06.007>.
- [29] Y. Ji, B. Xu, W. Gong, X. Zhang, X. Jin, W. Ning, Y. Meng, W. Yang, Y. Chen, Corrosion inhibition of a new Schiff base derivative with two pyridine rings on Q235 mild steel in 1.0 M HCl, *J. Taiwan Inst. Chem. Eng.* 66 (2016) 301–312, <https://doi.org/10.1016/j.jtice.2016.07.007>.
- [30] E.E. Elemike, H.U. Nwankwo, D.C. Onwuide, Synthesis and comparative study on the anti-corrosion potentials of some Schiff base compounds bearing similar backbone, *J. Mol. Liq.* 276 (2019) 233–242, <https://doi.org/10.1016/j.molliq.2018.11.161>.
- [31] M. Murmu, S.K. Saha, N.C. Murmu, P. Banerjee, Effect of stereochemical conformation into the corrosion inhibitive behaviour of double azomethine based Schiff bases on mild steel surface in 1 mol L⁻¹ HCl medium: an experimental, density functional theory and molecular dynamics simulation study, *Corros. Sci.* 146 (2019) 134–151, <https://doi.org/10.1016/j.corsci.2018.10.002>.
- [32] M. Rezaeivala, M. Ahmadi, B. Captain, S. Şahin-Bölükbaşı, A.A. Dehghani-Firoozabadi, R. William Gable, Synthesis, characterization, and cytotoxic activity studies of new N4O complexes derived from 2-((3-[2-morpholinoethylamino]-N3-[(pyridine-2-yl)methyl]propylimino) methyl)phenol, *Appl. Organomet. Chem.* 34 (2020), e5325, <https://doi.org/10.1002/aoc.5325>.
- [33] M. Rezaeivala, M. Ahmadi, B. Captain, M. Bayat, M. Saaidirad, S. Şahin-Bölükbaşı, B. Yıldız, R.W. Gable, Some new morpholine-based Schiff-base complexes; synthesis, characterization, anticancer activities and theoretical studies, *Inorg. Chim. Acta* 513 (2020), 119935, <https://doi.org/10.1016/j.ica.2020.119935>.
- [34] M. Rezaeivala, R. Golbedaghi, M. Khalili, M. Ahmad, K. Sayin, F. Chalabian, The different effects of metal ions on the synthesis of macrocyclic compounds: X-ray crystal structure, theoretical studies, antibacterial and antifungal activities, *Russ. J. Coord. Chem. Khimiya* 45 (2019) 142–153, <https://doi.org/10.1134/S1070328419020064>.
- [35] H. Keypour, M. Shayesteh, M. Rezaeivala, S. Dhers, F.Ö. Küp, M. Güllü, S. Ng, Mononuclear Ni(II) complexes of Schiff base ligands formed from unsymmetrical tripodal amines of differing arm lengths: spectral, X-ray crystal structural, antimicrobial and DNA cleavage activity, *J. Mol. Struct.* 1148 (2017) 568–576, <https://doi.org/10.1016/j.molstruc.2017.07.058>.
- [36] M. Rezaeivala, H. Keypour, S. Salehzadeh, R. Latifi, F. Chalabian, F. Katouzian, Synthesis, characterization and crystal structure of some new Mn(II) and Zn(II) macrocyclic Schiff base complexes derived from two new asymmetrical (N5) branched amines and pyridine-2-carbaldehyde or O-vaniline and their antibacterial properties, *J. Iran. Chem. Soc.* 11 (2014) 431–440, <https://doi.org/10.1007/s13738-013-0315-4>.

- [36] H. Keypour, A. Shoostari, M. Rezaeivala, F.O. Kup, H.A. Rudbari, Synthesis of two new N2O4 macrocyclic Schiff base ligands and their mononuclear complexes: spectral, X-ray crystal structural, antibacterial and DNA cleavage activity, *Polyhedron* 97 (2015) 75–82, <https://doi.org/10.1016/j.poly.2015.02.029>.
- [37] J. Haque, V. Srivastava, D.S. Chauhan, H. Lgaz, M.A. Quraishi, Microwave-induced synthesis of chitosan schiff bases and their application as novel and green corrosion inhibitors: experimental and theoretical approach, *ACS Omega* 3 (2018) 5654–5668, <https://doi.org/10.1021/acsomega.8b00455>.
- [38] M. Rezaeivala, S. Karimi, B. Tuzun, K. Sayin, Anti-corrosion behavior of 2-((3-(2-morpholino ethylamino) -N3-((pyridine-2-yl)methyl)propylimino)methyl)pyridine and its reduced form on Carbon Steel in Hydrochloric Acid solution: experimental and theoretical studies, *Thin Solid Films* 741 (2021), 139036, <https://doi.org/10.1016/j.tsf.2021.139036>.
- [39] X. Wang, H. Yang, F. Wang, An investigation of benzimidazole derivative as corrosion inhibitor for mild steel in different concentration HCl solutions, *Corros. Sci.* 53 (2011) 113–121, <https://doi.org/10.1016/j.corsci.2010.09.029>.
- [40] S.M.A. Hosseini, A. Azimi, The inhibition of mild steel corrosion in acidic medium by 1-methyl-3-pyridin-2-yl-thiourea, *Corros. Sci.* 51 (2009) 728–732.
- [41] M. Behpour, S.M. Ghoreishi, N. Mohammadi, N. Soltani, M. Salavati-Niasari, Investigation of some Schiff base compounds containing disulfide bond as HCl corrosion inhibitors for mild steel, *Corros. Sci.* 52 (2010) 4046–4057.
- [42] S. El Arrouji, K. Karrouchi, A. Berisha, K. Ismaily Alaoui, I. Warad, Z. Rais, S. Radi, M. Taleb, M. Ansar, A. Zarrouk, New pyrazole derivatives as effective corrosion inhibitors on steel-electrolyte interface in 1 M HCl: electrochemical, surface morphological (SEM) and computational analysis, *Colloids Surf. A Physicochem. Eng. Asp.* 604 (2020), 125325, <https://doi.org/10.1016/j.colsurfa.2020.125325>.
- [43] O. Dagdag, R. Hsissou, A. El Harfi, Z. Safi, A. Berisha, C. Verma, E.E. Ebenso, M. A. Quraishi, N. Wazzan, S. Jodeh, M. El Gouri, Epoxy resins and their zinc composites as novel anti-corrosive materials for copper in 3% sodium chloride solution: experimental and computational studies, *J. Mol. Liq.* 315 (2020), 113757, <https://doi.org/10.1016/j.molliq.2020.113757>.
- [44] H. Keypour, N. Rahpeyma, P. Arzhang, M. Rezaeivala, Y. Elerman, O. Buyukgungor, L. Valencia, Synthesis and characterization of Co(II), Ni(II), Zn(II) and Cu(II) complexes with a new tetraazamacrocyclic Schiff base ligand containing a piperazine moiety: X-ray crystal structure determination of the Co(II) complex, *Polyhedron* 29 (2010) 1144–1148, <https://doi.org/10.1016/j.poly.2009.12.005>.
- [45] M. Rezaeivala, Synthesis, characterization and theoretical studies of a new macrocyclic schiff-base ligand containing piperazine moiety and related Mn(II), Cu(II), Ni(II) and Cd(II) complexes, *Inorg. Chem. Res* 2 (2018) 85–92, <https://doi.org/10.22036/icr.2016.46261>.
- [46] B. El Ibrahim, K. El Mouaden, A. Jmiai, A. Baddouh, S. El Issami, L. Bazzi, M. Hilali, Understanding the influence of solution's pH on the corrosion of tin in saline solution containing functional amino acids using electrochemical techniques and molecular modeling, *Surf. Interfaces* 17 (2019), 100343, <https://doi.org/10.1016/j.surfin.2019.100343>.
- [47] A. Kosari, M.H. Moayed, A. Davoodi, R. Parvizi, M. Momeni, H. Eshghi, H. Moradi, Electrochemical and quantum chemical assessment of two organic compounds from pyridine derivatives as corrosion inhibitors for mild steel in HCl solution under stagnant condition and hydrodynamic flow, *Corros. Sci.* 78 (2014) 138–150, <https://doi.org/10.1016/j.corsci.2013.09.009>.
- [48] M.J. F.D.J. Frisch, G.W. Trucks, H.B. Schlegel, G.E. Scuseria, M.A. Robb, J. R. Cheeseman, G. Scalmani, V. Barone, B. Mennucci, G.A. Petersson, H. Nakatsuji, M. Caricato, X. Li, H.P. Hratchian, A.F. Izmaylov, J. Bloino, G. Zheng, J. L. Sonnenberg, M. Hada, M. Ehara, Gaussian 09, rev. D. 01, Gaussian Inc., Wallingford CT, 2009.
- [49] A.D. Becke, Density-functional thermochemistry. III. The role of exact exchange, *J. Chem. Phys.* 98 (1993) 5648–5652, <https://doi.org/10.1063/1.464913>.
- [50] P.J. Stephens, F.J. Devlin, C.F. Chabalowski, M.J. Frisch, Ab Initio calculation of vibrational absorption and circular dichroism spectra using density functional force fields, *J. Phys. Chem.* 98 (1994) 11623–11627, <https://doi.org/10.1021/j100096a001>.
- [51] K.B. Wiberg, Basis set effects on calculated geometries: 6-311++G** vs. aug-cc-pVDZ, *J. Comput. Chem.* 25 (2004) 1342–1346, <https://doi.org/10.1002/jcc.20058>.
- [52] D. Vautherin, D.M. Brink, Hartree-fock calculations with skyrme's interaction. I. Spherical nuclei, *Phys. Rev. C* 5 (1972) 626–647, <https://doi.org/10.1103/PhysRevC.5.626>.
- [53] E.G. Hohenstein, S.T. Chill, C.D. Sherrill, Assessment of the performance of the M05#2X and M06#2X exchange correlation functionals for noncovalent interactions in biomolecules, *J. Chem. Theory Comput.* 4 (2008) 1996–2000, <https://doi.org/10.1021/ct800308k>.
- [54] S. Satpati, S.K. Saha, A. Subasaria, P. Banerjee, D. Sukul, Adsorption and anti-corrosion characteristics of vanillin Schiff bases on mild steel in 1 M HCl: experimental and theoretical study, *RSC Adv.* 10 (2020) 9258–9273, <https://doi.org/10.1039/c9ra07982c>.
- [55] M.J. Frisch, G.W. Trucks H.B. Schlegel G.E. Scuseria M.A. Robb J.R. Cheeseman G. Scalmani V. Barone B. Mennucci G.A. Petersson Gaussian 09. 2009 1990 Gaussian, Inc. Wallingford, Ct, USA.
- [56] S. Karimi, A. Ghahreman, F. Rashchi, Kinetics of Fe(III)-Fe(II) redox half-reactions on sphalerite surface, *Electrochim. Acta* 281 (2018) 624–637, <https://doi.org/10.1016/j.electacta.2018.05.132>.
- [57] S. Karimi, A. Ghahreman, F. Rashchi, J. Moghaddam, The mechanism of electrochemical dissolution of sphalerite in sulfuric acid media, *Electrochim. Acta* 253 (2017) 58, <https://doi.org/10.1016/j.electacta.2017.09.040>.
- [58] A. Heidarpour, Z.S. Mousavi, S. Karimi, S.M. Hosseini, On the corrosion behavior and microstructural characterization of Al2024 and Al2024/Ti2SC MAX phase surface composite through friction stir processings, *J. Appl. Electrochem* (2021) 1–14, <https://doi.org/10.1007/s10800-021-01567-9>.
- [59] Y. Zhu, M.L. Free, R. Woollam, W. Durnie, A review of surfactants as corrosion inhibitors and associated modeling, *Prog. Mater. Sci.* 90 (2017) 159–223, <https://doi.org/10.1016/j.pmatsci.2017.07.006>.
- [60] H. Keypour, M. Rezaeivala, L. Valencia, P. Pérez-Lourido, Synthesis and characterization of some new Pb(II), Mn(II) and Ag(I) complexes with a pentaaza macrocyclic ligand containing a piperazine moiety, *Polyhedron* 28 (2009) 4096–4100, <https://doi.org/10.1016/j.poly.2009.09.031>.
- [61] Y. Zhang, L. Zhang, C. Zhou, Review of chemical vapor deposition of graphene and related applications, *Acc. Chem. Res.* 46 (2013) 2329–2339, <https://doi.org/10.1021/ar300203n>.
- [62] S.K. Saha, A. Dutta, P. Ghosh, D. Sukul, P. Banerjee, Adsorption and corrosion inhibition effect of Schiff base molecules on the mild steel surface in 1 M HCl medium: a combined experimental and theoretical approach, *Phys. Chem. Chem. Phys.* 17 (2015) 5679–5690.
- [63] B. Chugh, A.K. Singh, S. Thakur, B. Pani, H. Lgaz, I.M. Chung, R. Jha, E.E. Ebenso, Comparative investigation of corrosion-mitigating behavior of thiazazole-derived bis-schiff bases for mild steel in acid medium: experimental, theoretical, and surface study, *ACS Omega* 5 (2020) 13503–13520, <https://doi.org/10.1021/acsomega.9b04274>.
- [64] K. Vimal, R.B.V. Appa, Chemically modified biopolymer as an eco-friendly corrosion inhibitor for mild steel in a neutral chloride environment, *New J. Chem.* 41 (2017) 6278–6289, <https://doi.org/10.1039/c7nj00553a>.
- [65] H. Ashassi-Sorkhabi, Z. Ghasemi, D. Seifzadeh, The inhibition effect of some amino acids towards the corrosion of aluminum in 1 M HCl + 1 M H₂SO₄ solution, *Appl. Surf. Sci.* 249 (2005) 408–418, <https://doi.org/10.1016/j.apsusc.2004.12.016>.
- [66] R. Solmaz, G. Kardaş, M. Çulha, B. Yazici, M. Erbil, Investigation of adsorption and inhibitive effect of 2-mercaptothiazoline on corrosion of mild steel in hydrochloric acid media, *Electrochim. Acta* 53 (2008) 5941–5952, <https://doi.org/10.1016/j.electacta.2008.03.055>.
- [67] A. Sedik, D. Lerari, A. Salmi, S. Athmani, K. Bachari, I.H. Gecibesler, R. Solmaz, Dardagan Fruit extract as eco-friendly corrosion inhibitor for mild steel in 1 M HCl: electrochemical and surface morphological studies, *J. Taiwan Inst. Chem. Eng.* 107 (2020) 189–200.
- [68] N.K. Othman, S. Yahya, M.C. Ismail, Corrosion inhibition of steel in 3.5% NaCl by rice straw extract, *J. Ind. Eng. Chem.* 70 (2019) 299–310.
- [69] Z. Zhang, S. Chen, Y. Li, S. Li, L. Wang, A study of the inhibition of iron corrosion by imidazole and its derivatives self-assembled films, *Corros. Sci.* 51 (2009) 291–300.
- [70] H. Jafari, F. mohsenifar, K. Sayin, Corrosion inhibition studies of N,N'-bis(4-formylphenol)-1,2-Diaminocyclohexane on steel in 1 HCl solution acid, *J. Taiwan Inst. Chem. Eng.* 64 (2016) 314–324, <https://doi.org/10.1016/j.jtice.2016.04.021>.
- [71] P.C. Okafor, M.E. Ikpi, I.E. Uwah, E.E. Ebenso, U.J. Ekpe, S.A. Umoren, Inhibitory action of Phyllanthus amarus extracts on the corrosion of mild steel in acidic media, *Corros. Sci.* 50 (2008) 2310–2317, <https://doi.org/10.1016/j.corsci.2008.05.009>.
- [72] L. Tang, X. Li, Y. Si, G. Mu, G. Liu, The synergistic inhibition between 8-hydroxyquinoline and chloride ion for the corrosion of cold rolled steel in 0.5 M sulfuric acid, *Mater. Chem. Phys.* 95 (2006) 29–38, <https://doi.org/10.1016/j.matchemphys.2005.03.064>.
- [73] Ş. Erdoğan, B. Tüzün, Applications of the Effectiveness of Corrosion Inhibitors with Computational Methods and Molecular Dynamics Simulation, in: Applications of the Effectiveness of Corrosion Inhibitors with Computational Methods and Molecular Dynamics Simulation, IntechOpen, 2021, <https://doi.org/10.5772/intechopen.98968>.
- [74] M. El Faydy, H. About, I. Warad, Y. Kerroum, A. Berisha, F. Podvorica, F. Bentiss, G. Kaichouh, B. Lakhri, A. Zarrouk, Insight into the corrosion inhibition of new bis-quinolin-8-ols derivatives as highly efficient inhibitors for C35E steel in 0.5 M H₂SO₄, *J. Mol. Liq.* 342 (2021), 117333, <https://doi.org/10.1016/j.molliq.2021.117333>.
- [75] A. Ouass, M. Galai, M. Ouakki, E. Ech-Chihbi, L. Kadiri, R. Hsissou, Y. Essaadaoui, A. Berisha, M. Cherkaoui, A. Lebkiri, E.H. Rifi, Poly(sodium acrylate) and Poly (acrylic acid sodium) as an eco-friendly corrosion inhibitor of mild steel in normal hydrochloric acid: experimental, spectroscopic and theoretical approach, *J. Appl. Electrochem.* 51 (2021) 1009–1032, <https://doi.org/10.1007/s10800-021-01556-y>.